



***Finite Element Analyses of the
XPD BRC2 Collimator***

(Vault File: 'PD-XPD-BL-FMB_AZM0008-FMB_AZM0008_Rev3-CALC-AZM0008.docx')

By

Steven W. O'Hara

NSLS-II

Brookhaven National Laboratory

2018 March 05

Summary

Steady-state thermal, static structural, and coupled thermal-structural finite element analyses were performed on the Bremsstrahlung Collimator (BMCR2) of the X-ray Powder Diffraction (XPD) Beamline located at 28-ID-2 at the NSLS-II. The case considered here is a beam miss-steer that causes the worst case beam position to partially hit the Tungsten block at normal incidence with a total deposited power of about 1.6 kW. This condition can only be caused by several improbable events occurring upstream simultaneously, and escaping detection.

Thermal results show that the temperature of the Tungsten components of the collimator is well below the melting temperature (about half). However, the aluminum support block has significant areas where the temperature exceeds the melting temperature, and the aluminum support plate has some areas where the temperature exceeds the melting temperature.

Static structural results show that in the event the beam is miss-steered into one of the four stainless steel support rods, causing rod failure, the three remaining rods can easily support the tungsten blocks with minimal additional deflection.

Coupled thermal-structural results show that, due to thermal expansion, the location of the Tungsten block aperture shifts approximately 0.58 mm horizontally, and 2.96 mm vertically. This shift does not significantly alter the thermal results.

Table of Contents

Summary	2
1. Introduction	4
2. Analysis Parameters and Setup	5
2.1 Model	5
2.2 Material Properties	6
2.3 Emissivity.....	6
2.3.1 Tungsten.....	6
2.3.2 Aluminum.....	6
2.3.3 Stainless Steel	7
2.4 Power Distribution and Thermal Loading	7
2.5 Mechanical Environment	9
2.6 Thermal Environment: Convective Cooling & Radiation	10
2.7 FEA Mesh	10
3. Results	11
3.1 Results Summary.....	11
3.2 Thermal Results.....	11
3.3 Static Structural Results	13
3.4 Coupled Thermal-Structural Results	16
4. Conclusions	17
Appendix A: Report “FMB-O- AZM0008 Rev3 BRC2 wo FMK2 Report Rev0”	18

1. Introduction

The scope of this project is to perform steady-state thermal, static structural, and coupled thermal-structural finite element analyses on the Bremsstrahlung Collimator (BMCR2) of the X-ray Powder Diffraction (XPD) Beamline located at 28-ID-2 at the NSLS-II. The collimator is 33.37 m from the source and the total power in the beam is 7.95 kW.

A model of the full collimator assembly is shown in Figure 1(A) and a detailed view of the internal components is shown in Figure 1(B). The model is stored in Vault as “PD-XPD-BL-FMB_AZM0008-FMB_AZM0008_Rev3-AZM0008.stp.” Relevant individual components and their corresponding materials are indicated. It is not obvious from Figure 1, but the stainless steel support rods are connected to the top of the vacuum chamber and hang freely without being supported from the bottom.

The thermal case considered here is a beam miss-steer that causes the worst case beam position to partially hit the Tungsten block at normal incidence with a total deposited power of about 1.6 kW. The remaining beam continues to pass through the aperture. It is required to know if the temperature of the Tungsten block exceeds the melting temperature. Details of the power and loading position are discussed in a later section. This condition can only be caused by several improbable events occurring upstream simultaneously, and escaping detection. More details are given in report “FMB-O- AZM0008 Rev3 BRC2 wo FMK2 Report Rev0.docx”, which is included as Appendix A.

If this severe miss-steer occurs, it is also possible that the beam strikes either one of the stainless steel support rods on the upstream side of the collimator. If this happens, the worst case is that the beam burns through the rod and it fails to support any load. It is required to know if the three remaining rods can support the Tungsten and Aluminum components with acceptable deflection. Static structural analyses with gravity will be done to determine this. The baseline case using all four rods will be analyzed to determine the starting point for any further deformation.

Finally, a coupled steady-state thermal and static structural analysis will be done to determine the magnitude of the thermal expansion from the anticipated high temperatures.

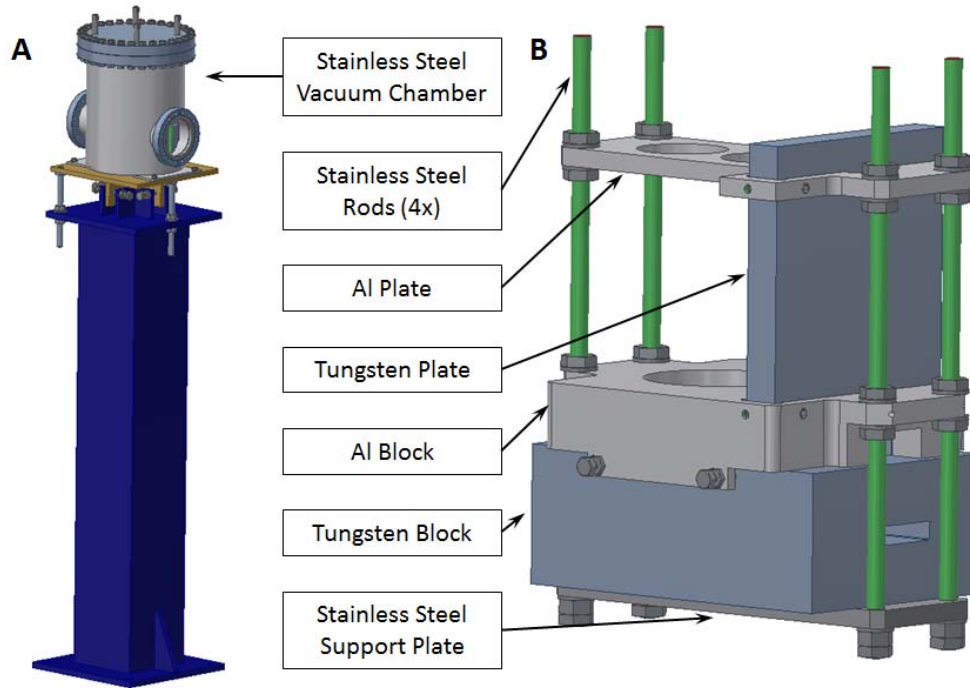


Figure 1. XPD Collimator BRC2; "AZM0008.stp".
(A) Full Assembly; (B) Detail Showing Inner Components and Material Identification

2. Analysis Parameters and Setup

2.1 Model

Figure 2 shows the model prepared for FEA in ANSYS. The model has been de-featured; only the components relative to the finite element analysis have been retained and extraneous features have been suppressed.

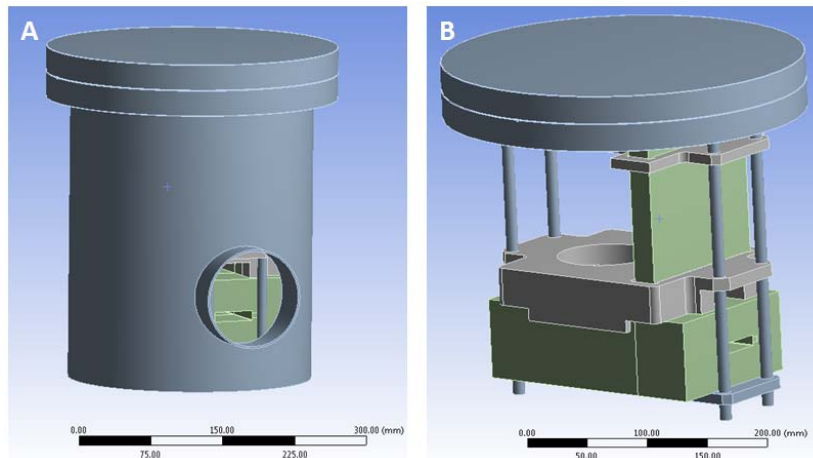


Figure 2. XPD Collimator BRC2 Prepared for FEA
(A) Full ANSYS Model; (B) Detail Showing Inner Components

2.2 Material Properties

The component materials are identified in Figure 1 and the material properties used in this analysis are listed below in Table 1. The reference temperature is 22.0°C (ambient). Emissivity is discussed in the next section.

Material	Density [kg/m ³]	Young's Modulus [Pa]	Poisson's Ratio	Coefficient of Thermal Expansion [1/°C]	Thermal Conductivity [W/m-°C]
Tungsten	19300	4.00E+11	0.28	4.4E-6	163.3
Stainless Steel	7750	1.93E+11	0.31	1.7E-5	15.1
Aluminum Alloy	2770	7.10E10	0.33	2.3E-5	165.0

Table 1. Material Properties

2.3 Emissivity

2.3.1 Tungsten

The following temperature dependent emissivity data for unoxidized Tungsten (Table 2) was taken from the Mikron Instrument Company, Inc. web page. The web page lists the following references: (1) 'Handbook of Chemistry and Physics', Chemical Rubber Publishing Co., Cleveland, Ohio; (2) 'DMIC Report 177', Battelle Memorial Institute; (3) 'Thermal Radiation Survey', Honeywell Research Center. This data was verified by comparing with other website data.

Temperature [°C]	Emissivity
25	0.024
100	0.032
500	0.071
1000	0.15
1500	0.23
2000	0.28

Table 2. Temperature Dependent Emissivity of Tungsten

2.3.2 Aluminum

An emissivity of 0.090 is used for aluminum based on the data in Table 3. The information comes from the same source as that of Tungsten above, and was verified by comparing with other website data.

Condition	Temperature [°C]	Emissivity
Polished	100	0.095
Unoxidized	500	0.060
Oxidized	600	0.190
Commercial Sheet	100	0.090

Table 3. Emissivity of Aluminum

2.3.3 Stainless Steel

A generally accepted value of emissivity of stainless steel is 0.5 (“The Emissivity of Stainless Steel in Dairy Plant Thermal Design”, A. J. Baldwin & J. E. Lovell-Smith, Journal of Food Engineering 17, 281-289 (1992)),

2.4 Power Distribution and Thermal Loading

The power distribution was provided by Oleg Tchoubar as “DW100_PowDens.xlsx” and is summarized in Table 4 and plotted in Figure 3. This power distribution was calculated in a plane normal to the central axis of the 28-ID source distribution, at a distance corresponding to the upstream face of the XPD FM2K Mask (33.11mm). For convenience, this distribution was also used as the input power distribution on the Bremsstrahlung collimator BRC2, which is located at 33.37 m from the source, just slightly downstream of FM2K. This is a conservative approximation.

Description	Total Power [W]	Max Normal Power Density [W/mm ²]	Power Incident on Tungsten Block [W]
Total Emitted Power	7947.8	49.29	≈1600.0

Table 4. Power Distribution Details



Figure 3. Normal Power Distribution (Data Provided by Oleg Tchoubar as “DW100_PowDens.xlsx.”)

Figure 4 shows a detail of the relative positions of the Tungsten Block Aperture, PPS Fan, Max Tolerance Beam, and Nominal Beam for the worst case beam position. The worst case beam position will result in the highest temperature on the Tungsten block. There is less material on the right hand side of the Tungsten block (looking downstream) so the worst case position is on this side. Figure 5 shows the beam position on the Tungsten block. Note that in Figures 4 and 5 the stainless steel support rods are not shown.

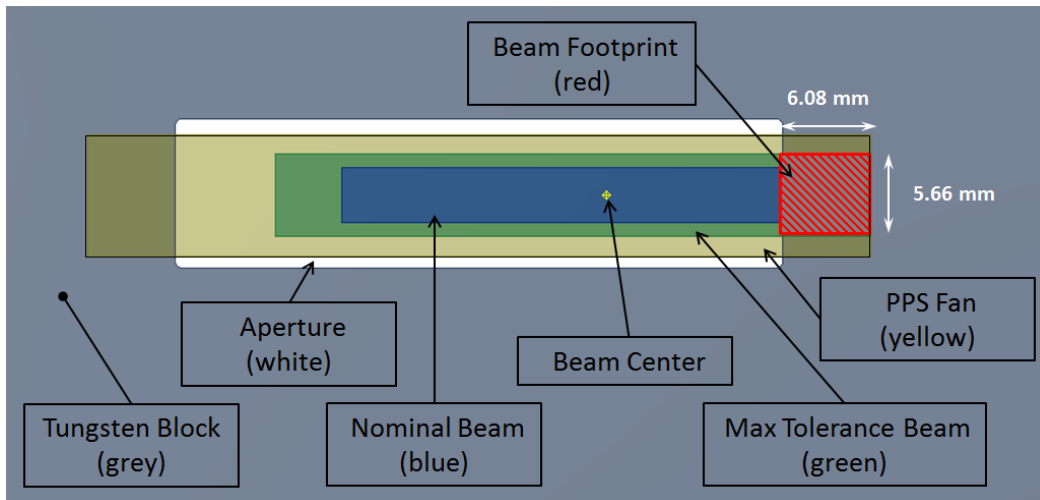


Figure 4. Detail of Tungsten Block Showing Relative Positions of the PPS Fan, Max Tolerance Beam, Nominal Beam, and Beam Footprint in the Worst Case Beam Position

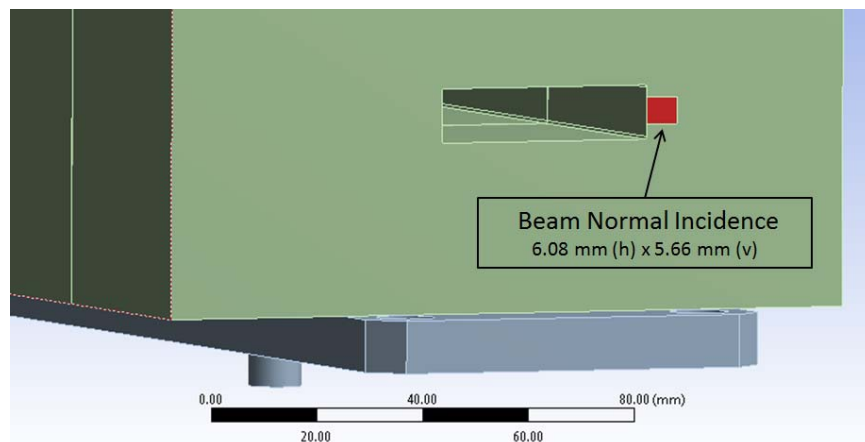


Figure 5. Beam Footprint on the Tungsten Block (detail of model).

Figure 6 again shows a detail of the relative positions of the Tungsten Block Aperture, PPS Fan, Max Tolerance Beam, and Nominal Beam for the worst case beam position, but also includes the two stainless steel support rods on the upstream side of the collimator (refer to Figure 4 above for more

information). It is clear that in the worst case beam position, the beam first strikes the stainless steel rod before hitting the Tungsten block. It is assumed that the beam will burn thru the rod rather quickly (stainless steel has poor thermal conductivity, which results in higher temperature, and a melting temperature much less than Tungsten). The focus of the thermal analysis is the steady-state condition after this happens. In the unlikely event that the rod does not burn thru, the thermal case analyzed would be very conservative.

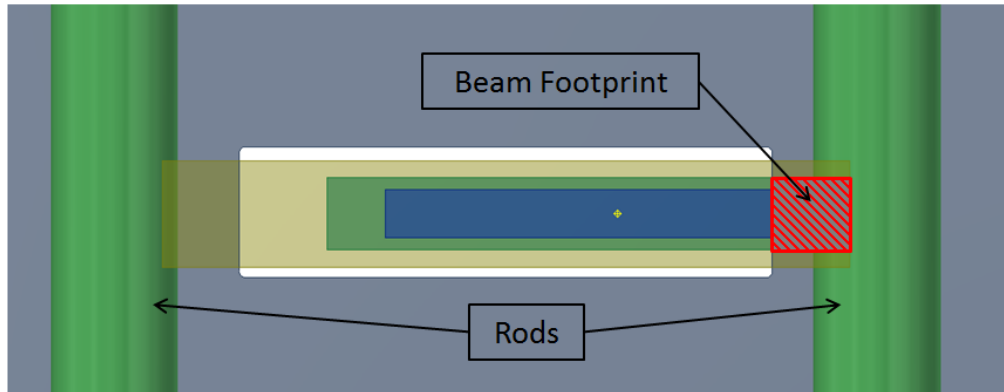


Figure 6. Detail of Tungsten Block Showing Relative Positions of the PPS Fan, Max Tolerance Beam, Nominal Beam, Beam Footprint in the Worst Case Beam Position, and also Two Upstream Rods.

As shown in Figure 6, the PPS Fan overlaps the stainless steel support rods, so it is possible that either rod can be hit by the beam. Static structural analyses with gravity will be done for each case, assuming the rod hit can no longer support any weight and only the remaining three rods support the Tungsten.

2.5 Mechanical Environment

Standard Earth Gravity is used for the static structural analysis. A fixed support boundary condition is applied to the top of the vacuum chamber. See Figure 7. For the coupled thermal-structural analysis the top surface is allowed to expand in-plane.

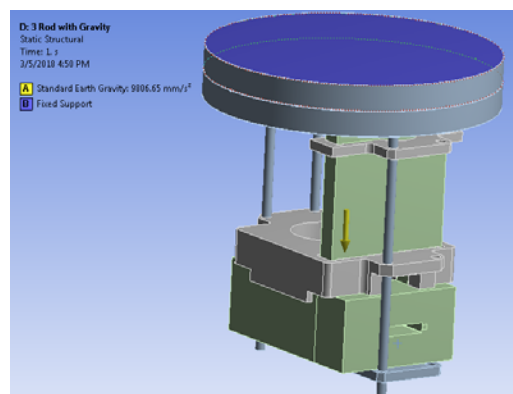


Figure 7. Mechanical Boundary Conditions

2.6 Thermal Environment: Convective Cooling & Radiation

In addition to thermal conduction between bodies, “Surface-to-Surface” thermal radiation occurs between all components within the vacuum vessel, including the vacuum vessel inner surface. The outer vacuum vessel surface has radiation type “Radiation to Ambient”, with a standard ambient temperature of 22°C.

The outer surface of the vacuum vessel also has natural convection to stagnant air. The ANSYS Engineering Data Library – Convection of Cylinder is used for the analysis. The convection film coefficient is temperature dependent.

2.7 FEA Mesh

Figure 8(A) shows the finite element mesh of the internal components of the BRC2 vacuum vessel and Figure 8(B) shows a close-up of the area around the beam footprint on the front face of the Tungsten block. The vacuum vessel and one of the 4 rods are not shown to allow the mesh to be seen more easily.

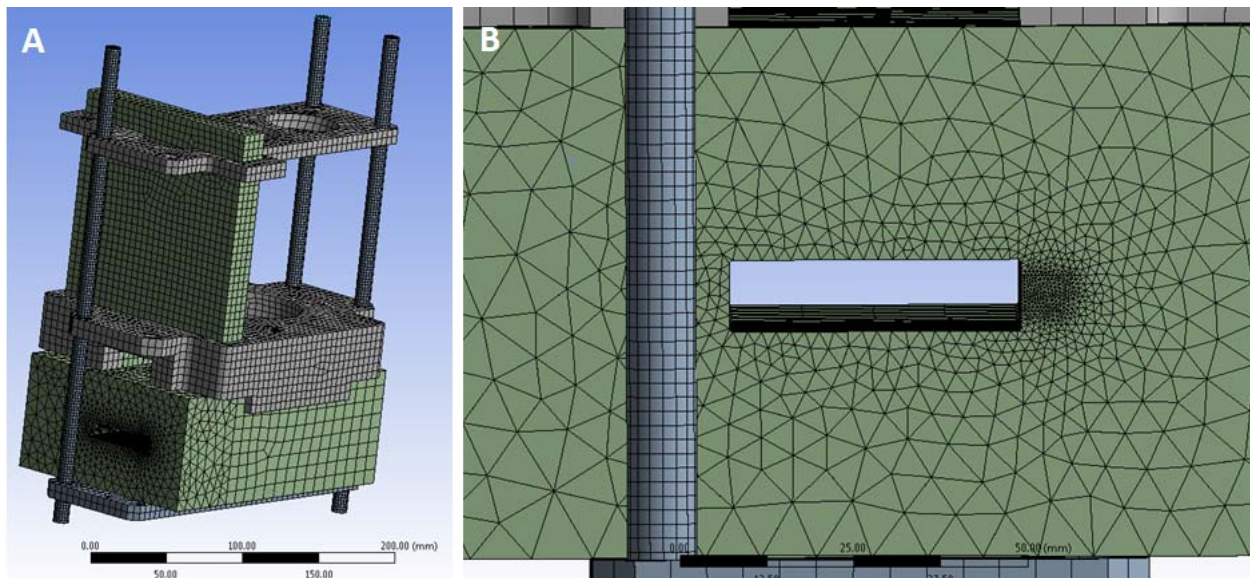


Figure 8. Finite Element Mesh: (A) BRC2 Inner Components; (B) Close-up of Heat Load Area. (One of the 4 rods is not visible.)

3. Results

3.1 Results Summary

Table 5 shows a summary of the steady-state thermal results. It is important to note that most of the aluminum block and part of the aluminum plate exceed the melting temperature of the aluminum alloy used. Graphical results of the thermal analysis are presented in section 3.2 and the static structural results are discussed in section 3.3. The coupled thermal-structural results are presented in section 3.4.

Component	Maximum Temperature [°C]	Melting Temperature [°C]
Tungsten Block	1749.6	≈ 3400
Tungsten Plate	707.0	≈ 3400
Aluminum Block	713.7	≈ 555-570
Aluminum Plate	600.2	≈ 555-570
Stainless Steel Plate	746.8	≈ 1400
SS Vacuum Chamber – Inner Surface	384.1	≈ 1400
SS Vacuum Chamber – Outer Surface	381.1	≈ 1400

Table 5. Thermal Results Summary

3.2 Thermal Results

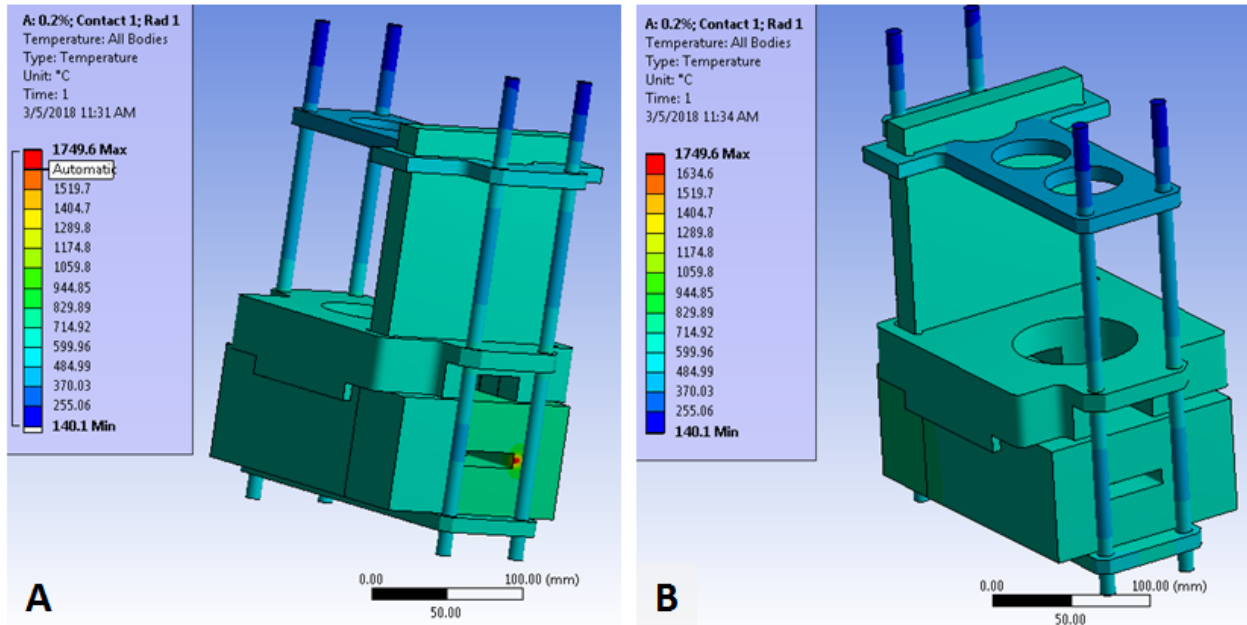


Figure 9. Temperature Distribution of the Internal Components

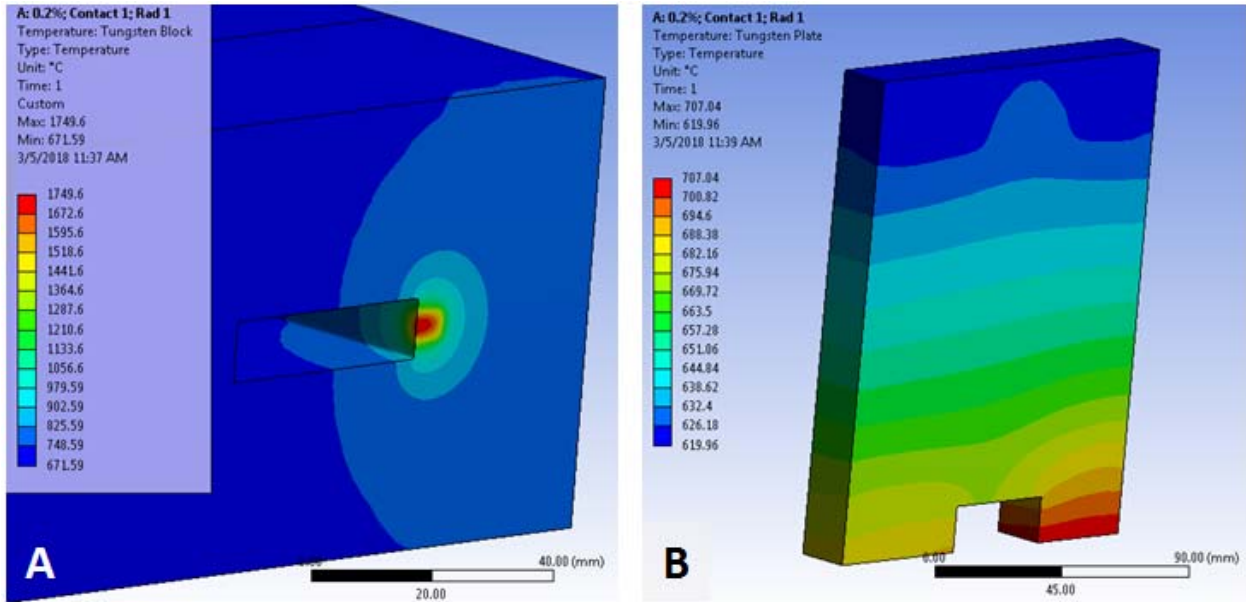


Figure 10. Temperature Distribution of the Tungsten Components
 (A) Tungsten Block; (B) Tungsten Plate

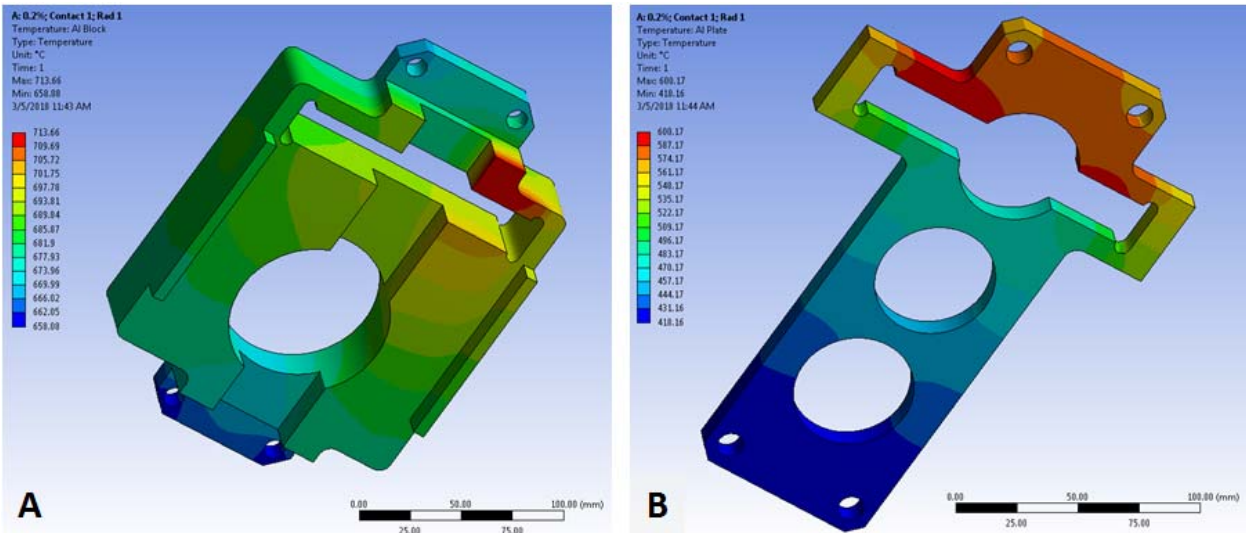
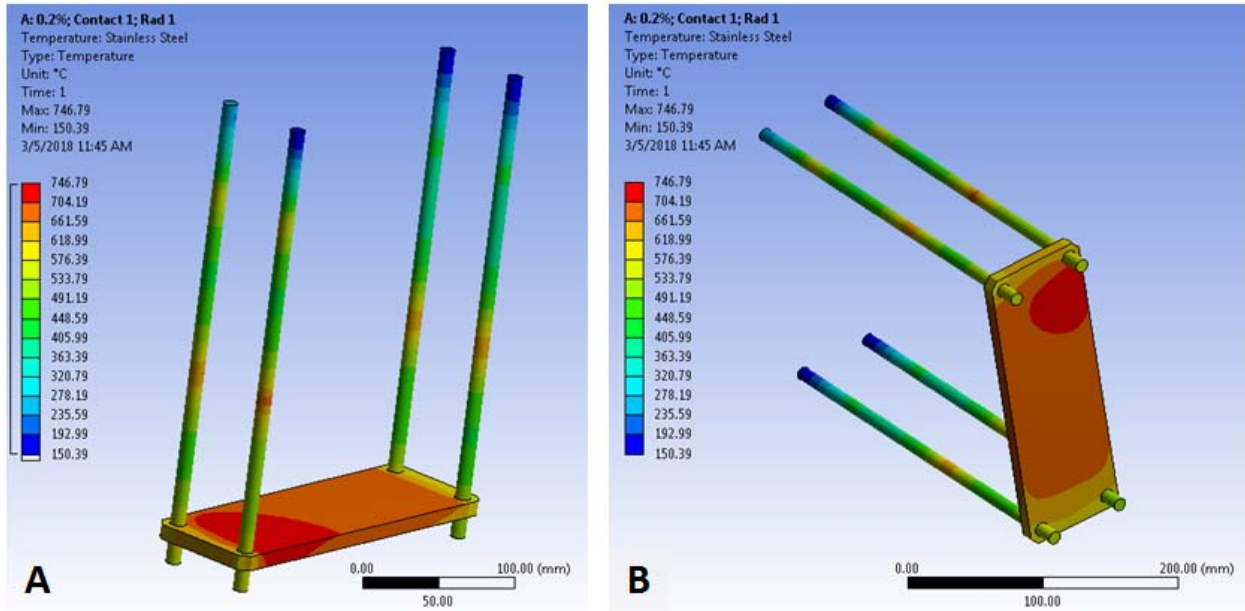


Figure 11. Temperature Distribution of the Aluminum Components
 (A) Aluminum Block; (B) Aluminum Plate



**Figure 12. Temperature Distribution of the Stainless Steel Components
(A) View Looking Down; (B) View Looking Up**

3.3 Static Structural Results

Figure 13 shows the total deformation of the assembly with all four stainless steel rods in place. This is the baseline, which is used as an initial reference from which further deformation due to a rod failure is measured. Figure 14 shows the total deformation for the case of the inboard rod missing. Figure 15 shows the total deformation for the case of the outboard rod missing. The maximum total deformation of 0.021 mm is at the outboard side of the aperture, which occurs when the outboard rod is eliminated. Figure 16 shows two detail views of the stress at the maximum total deformation case (Total Deformation with Outboard Rod Removed). Table 6 shows a summary of the results.

Configuration	Vertical Deformation [mm]		Total Deformation [mm]	
	Inboard Side of Aperture	Outboard Side of Aperture	Inboard Side of Aperture	Outboard Side of Aperture
4-Rod (Initial Position)	1.68E-3	2.33E-3	3.86E-3	4.21E-3
3-Rod (Inboard rod removed)	5.83E-3	n/a	1.06E-3	n/a
3-Rod (Outboard rod removed)	n/a	8.82E-3	n/a	2.50E-2
Total Deformation from Initial Position	0.004	0.007	0.003	0.021

Table 6. Structural Results Summary

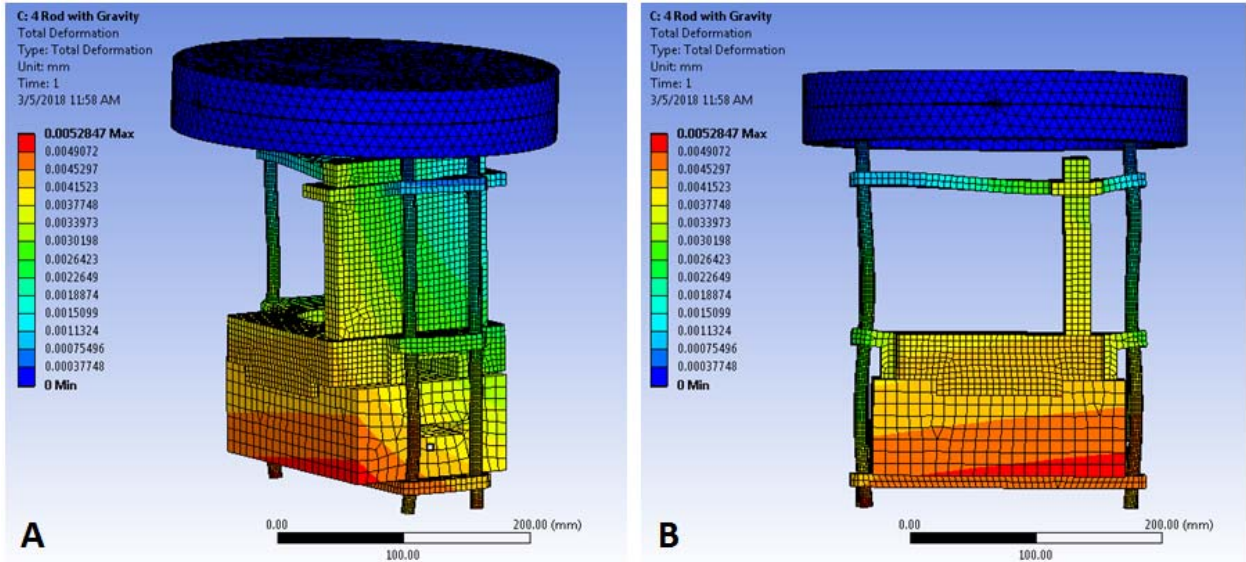


Figure 13. Total Deformation of the 4-Rod Case (Baseline)
(A) Front-Outboard View; (B) Outboard Side

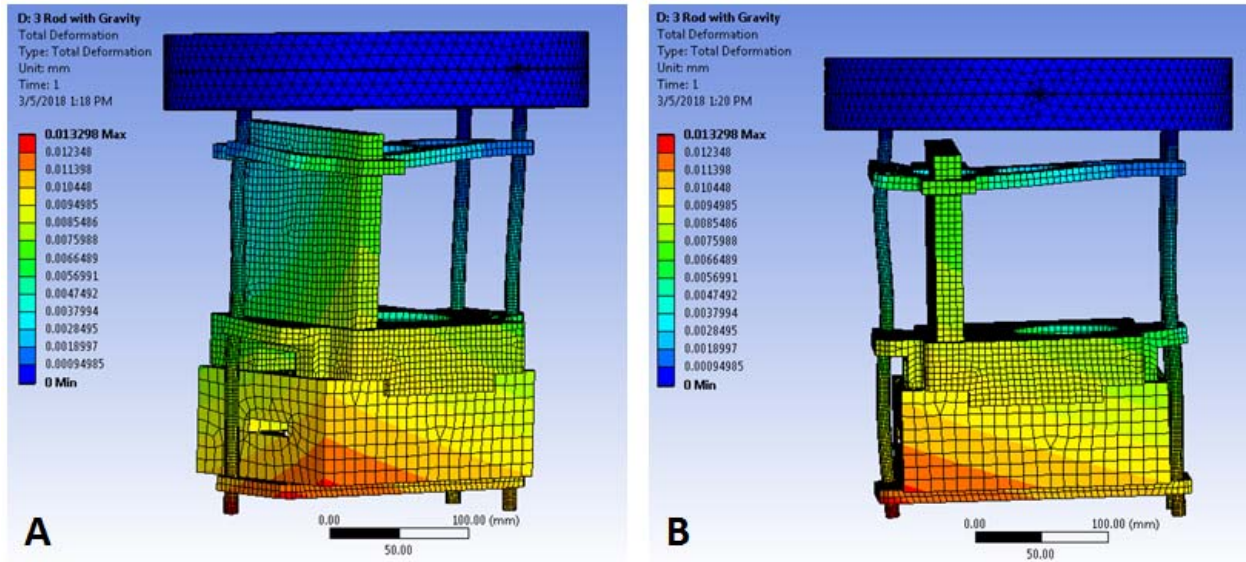
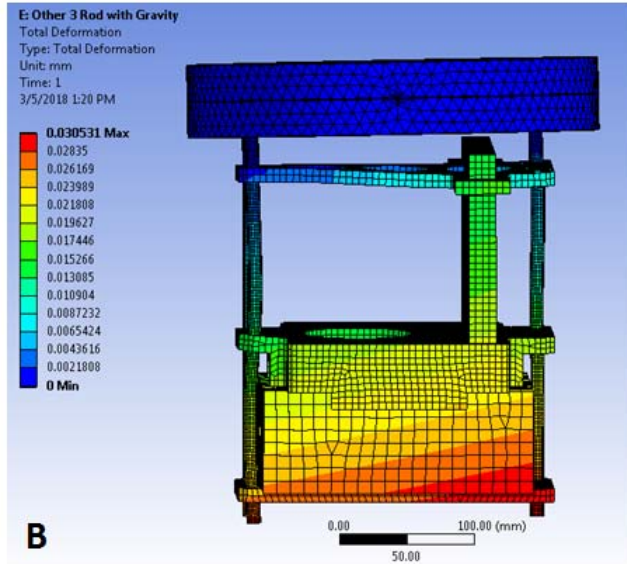
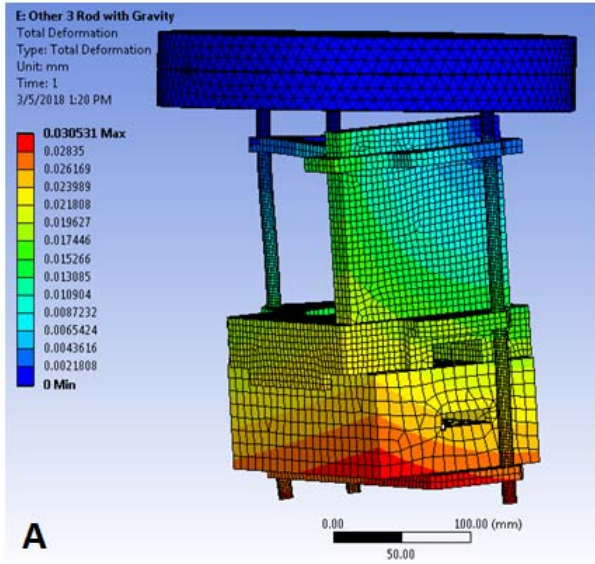


Figure 14. Total Deformation of the First 3-Rod Case
(A) Front-Inboard View; (B) Inboard Side



**Figure 15. Total Deformation of the Second 3-Rod Case
 (A) Front-Outboard View; (B) Outboard Side
 (B)**

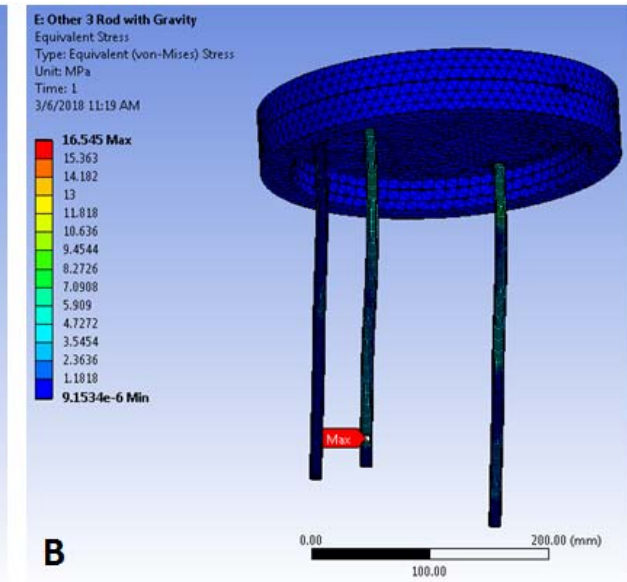
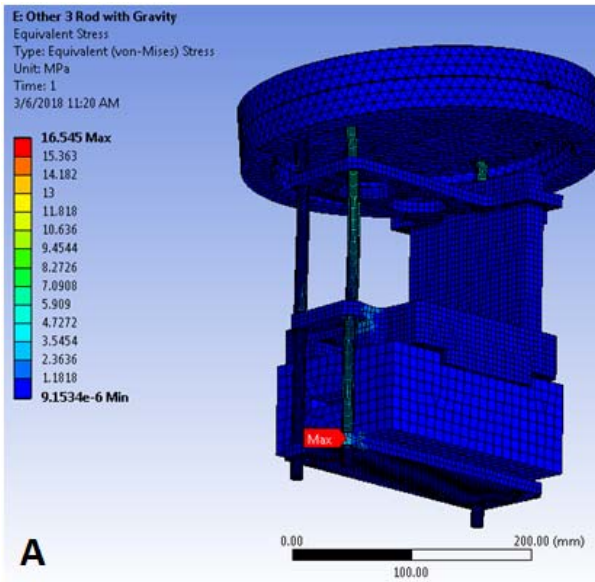


Figure 16. Equivalent Stress Distribution for Maximum Deflection Case. (A) & (B) Detail Views.

3.4 Coupled Thermal-Structural Results

Results from the coupled thermal-structural analysis show that thermal deformation causes the aperture to shift approximately 0.58 mm outboard horizontally, and 2.96 mm vertically downward. This shift does not significantly alter the thermal results. Total deformation contour plots are shown in Figure 17. Obviously, the results for the aluminum components that are expected to melt are not meaningful. The important results here are the thermal expansion of the stainless steel and Tungsten components.

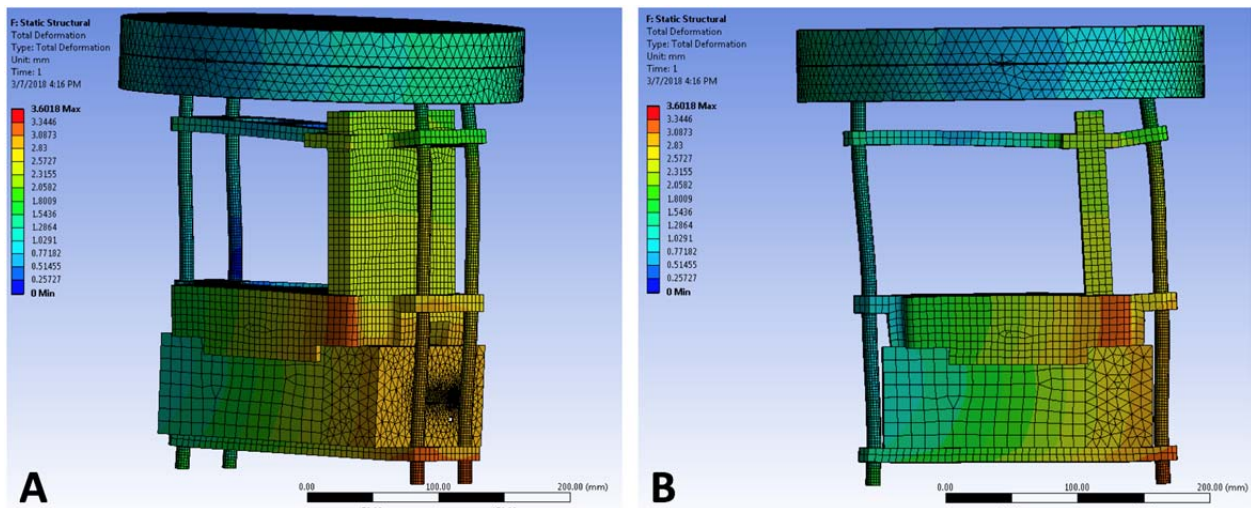


Figure 17. Total Deformation from Thermal Expansion. (A) & (B) Detail Views.

4. Conclusions

Steady-state thermal and static structural finite element analyses were performed on the Bremsstrahlung Collimator (BMCR2) of the X-ray Powder Diffraction (XPD) Beamline located at 28-ID-2 at the NSLS-II. The collimator is 33.37 m from the source. The case considered here is a beam miss-steer that causes the worst case beam position to partially hit the Tungsten block at normal incidence with a total deposited power of about 1.6 kW. This condition can only be caused by several improbable events occurring upstream simultaneously, and escaping detection.

Thermal results show that the temperature of the Tungsten components of the collimator is well below the melting temperature (about half). However, the aluminum support block has significant areas where the temperature exceeds the melting temperature, and the aluminum support plate has some areas where the temperature exceeds the melting temperature (see Appendix A for a discussion of the implications of this, which concludes that the BRC2 collimator remains functional).

Structural results show that in the event the beam is miss-steered into one of the four support rods, causing rod failure, the three remaining rods can easily support the tungsten blocks with minimal deflection and stress. The maximum deflection at the aperture is 0.02 mm and the maximum stress is 16.5 MPa.

The coupled thermal-structural results show that due to thermal expansion the location of the Tungsten block aperture shifts approximately 0.58 mm horizontally, and 2.96 mm vertically. This shift does not significantly alter the thermal results.

Appendix A: Report “FMB-O- AZM0008 Rev3 BRC2 wo FMK2 Report Rev0”

Appendix A contains report “FMB-O- AZM0008 Rev3 BRC2 wo FMK2 Report Rev0.docx”, written by Ed Hass and dated 08 March 2018.

REPORT:

XPD FMK2 FAILURE CONSEQUENCES

Revision 0

08 March 2018

PDF beamline working group, including;

M. Abeykoon

E. Dooryhee

E. Haas

S. O'Hara

C. Stelmach

Introduction:

This preliminary report considers the consequences of failure for XPD Fixed Mask 2 (FMK2; reference Design Review, June 09, 2014¹) located inside enclosure 28-ID-A at Z = 33.11 m from the damping wiggler source point, just downstream of the XPD Double Laue Monochromator (DLM). It is a follow-up to the Radiation Safety review that took place on 2/13/2018 and is a response to Andrew Ackerman's email dated 2/14/2018. Two action items were requested:

1. Re-do the ray traces without taking credit for Fixed Mask 2 to determine if beam can propagate past the Tungsten collimator and illuminate something downstream.
2. Complete Finite Element Analysis (FEA) for Bremsstrahlung collimator 2 (BRC2) to assure the tungsten AND the mechanical attachment for that collimator can handle the XPD beam heat load without the diamond windows and fixed mask 2.

This document addresses both of these actions. The results herein were presented to the Radiation Safety Committee on 2/28/2018.

Status:

1. The XPD Ray Trace drawing (PD-XPD-RAYT-0001) was updated to show rays not trimmed by FMK2. As of 28 February 2018, this drawing is in review.
2. XPD Bremsstrahlung collimator 2 (BRC2) was analyzed using the as-built configuration supplied by FMB/Oxford for the XPD beamline assuming Fixed Mask 2 (FMK2) is not trimming the XPD Maximum Synchrotron Fan. The preliminary findings are provided herein. A more complete FEA report is being filed by Steve O'Hara in Vault (reference PD-XPD-BL-FMB_AZM0008-FMB_AZM0008_Rev3-CALC-AZM0008).

Findings:

1. The XPD/PDF Ray Trace drawing now includes a view showing the path of the Maximum Synchrotron Horizontal fan without mask FMK2. Mask FMK2 only trims the XPD white beam horizontally; it does not trim the Vertical Maximum Synchrotron fan. Under these conditions, most of the additional beam hits the BRC2 large tungsten block. A small amount of beam proceeds to the white beam stop, some of which hits the white beam stop vacuum vessel. Figures 2, 3, and 6 show the projections and effects of the Max Synchrotron Fan on BRC2 and on the white beam stop vacuum vessel.
2. Analyses were performed to consider the effects of the added heat load. The following assumptions are made:

¹ Supporting documentation for 'Design Review for CSX and XPD PPS Masks', Monday, June 09, 2014 is posted at <https://ps.bnl.gov/phot/BeamlineSupportDocs/Forms/AllItems.aspx?RootFolder=%2Fphot%2FBeamlineSupportDocs%2FXPD%20PPS%20Mask>. FMK2 was hydrostatically pressure tested to 150 PSI, but not helium vacuum checked.

- Synchrotron beam is fully mis-steered horizontally within the PPS max fan envelope to the worst-case location
 - both of the diamond windows located upstream of the FMK2 are fully destroyed (without tripping vacuum or thermal sensors)
 - the five SiC window (total thickness = 7.4mm) are fully destroyed (also without tripping vacuum or thermal sensors)
- Note: these actuated filters are forced into the beam path by the PLC software, based on the value of the ring current.
- the first DLM crystal is destroyed (also without tripping vacuum or thermal sensors).
 - XPD white beam is not trimmed by FMK2 (i.e. FMK2 is damaged, also without tripping any vacuum sensors).

The occurrence of these five failures allows 1.6 kW of white beam to impact the large tungsten Bremsstrahlung Collimator 2 (BRC2) block which is located just downstream of the DLM (Fig. 2). Also, a small amount of this additional white beam proceeds downstream to the white beam stop (STW) and its' vacuum vessel. Assuming beam impact continues long enough to reach steady state conditions, the preliminary analyses show:

- the large tungsten collimator block reaches a maximum temperature of $\sim 1750^{\circ}\text{C}$ and the tungsten plate reaches a maximum temperature of $\sim 707^{\circ}\text{C}$ (melting point: $\sim 3400^{\circ}\text{C}$) (Fig. 3). Material certification was provided by FMB-O and is included herein (Fig. 7). The BRC2 tungsten materials meet the 18 g/cc density requirement and LT-C-XFD-SPC-XPD-BLC-001 specifications (i.e. no porosity or high vapor pressure elements).
- the 304/316 stainless steel support plate (AAC0170) reaches a maximum temperature of 747°C (melting point: $\sim 1400^{\circ}\text{C}$) (Fig. 4)
- the 6082-T6 aluminum block (ACC0078) directly above the large tungsten block (which does not support the large tungsten collimator block) experiences melting
- the 5083/6082 aluminum upper plate (AAC0170) that holds the tungsten plate in place reaches a maximum temperature of $\sim 600^{\circ}\text{C}$ and experiences partial melting (melting point: $570/555^{\circ}\text{C}$ respectively)
- one of the four stainless steel rods supporting the large tungsten collimator block is significantly damaged (not shown; structural analyses *conservatively* consider three threaded support rods whereas thermal analyses use four rods for maximum heat transfer). The case where beam hits both the tungsten block and a stainless steel rod was not analyzed due to the poor thermal conductivity ($163\text{-}173\text{ W/m-K}$ for tungsten versus $12\text{-}45\text{ W/m-K}$ for stainless steel) and smaller cross-sectional area for the support rods. The most conservative cases only were considered. Once the conduction paths are not providing full heat transfer, the temperature in the support plates is expected to drop, thus enough structure should be retained to hold the upper tungsten plate.

- The lower BRC2 tungsten collimator block continues to be supported if either one of the two stainless steel support rods is fully destroyed.
- Minimal movement (~ 0.02 mm) of the large BRC2 tungsten block occurs if either one of the two upstream stainless steel supports rods is completely destroyed.
- the outer surface of the BRC2 vacuum vessel heats up to 381°C at a location that is largely inaccessible. (Fig. 5)
- The small amount of white beam passing BRC2 and not impacting the white beam stop conservatively raises the white beam stop (STW) upstream vacuum vessel flange temperature locally to 929°C . (Fig. 6)

Conclusion:

A final and more detailed FEA report is being issued, however based on the above results, we believe it is safe to operate the XPD and PDF beamlines using the present FMK2 to trim the Maximum Synchrotron fan at 500 milliamps ring current. Although the analyses show the aluminum plates above the BRC2 large tungsten collimator experience melting, the large collimator block would continue to be supported and therefore remain functional. In the accidental scenario presented in this document, all beam-power-mitigating components are assumed to fail without tripping any vacuum or thermal sensors; therefore the first crystal of the DLM would also be destroyed. Hence there can be no XPD monochromatic beam passing 50 mm above the XPD white beam through the tungsten plate opening just above the large tungsten block.

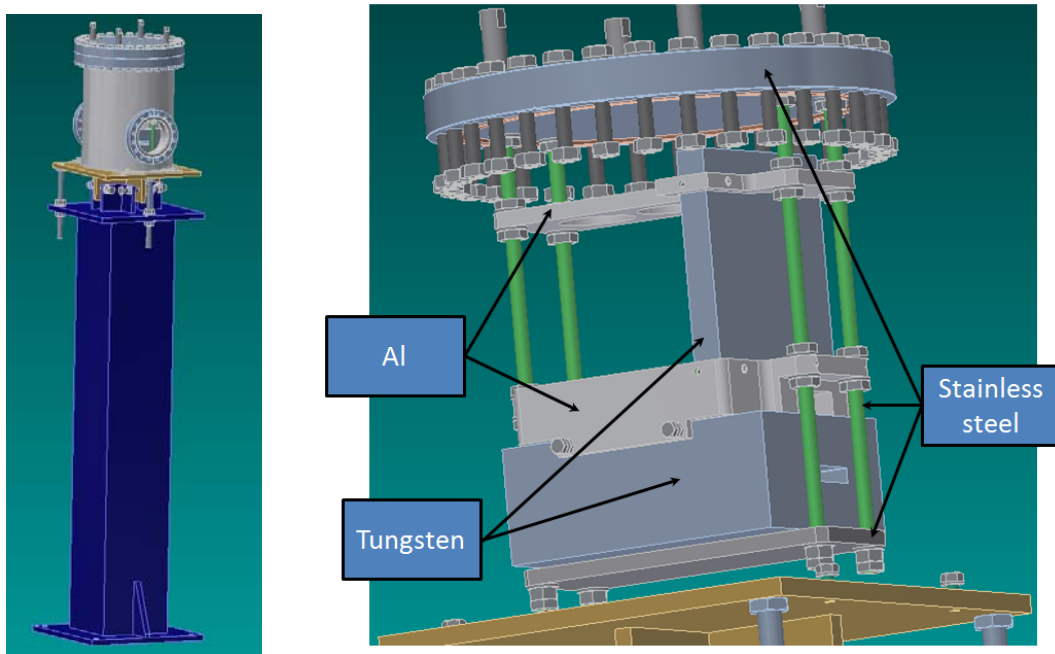


Figure 1: BRC2 (a) external view with support stand and (b) showing internal components

Finite Element Analysis Results

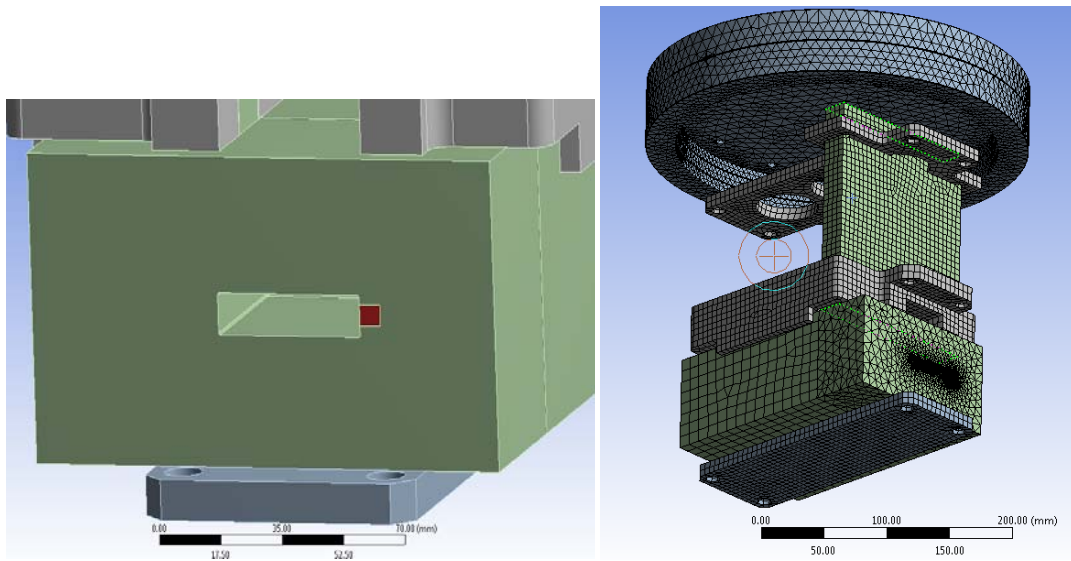


Figure 2: Views (a) looking downstream at XPD BRC2 (AZM0008 Rev3) showing white beam impact without FMK2, and (b) meshed elements (both views have the BRC2 vacuum vessel removed)

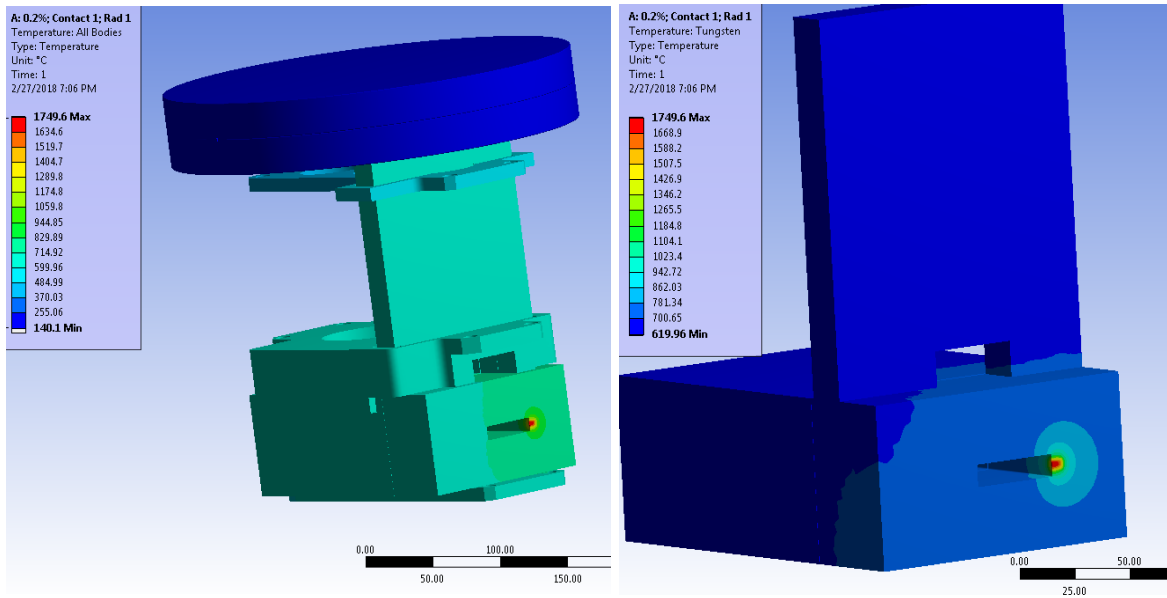


Figure 3: Thermal Analysis results of XPD BRC2 (AZM0008 Rev3) internal components, (vacuum vessel removed)

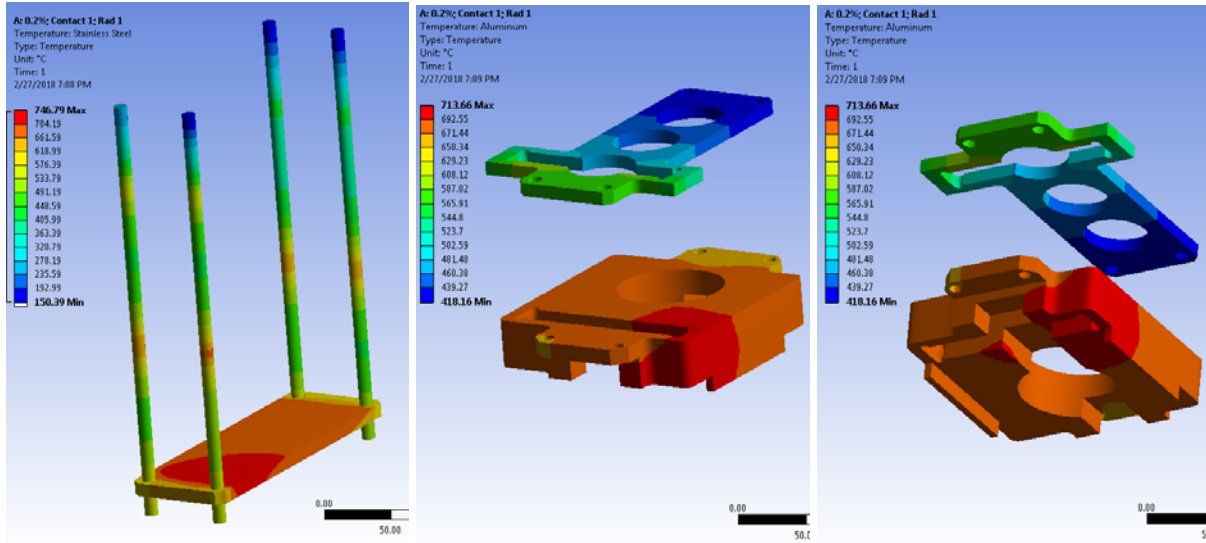


Figure 4: Thermal Analysis results of XPD BRC2 (AZM0008 Rev3) internal plates, (vacuum vessel removed)

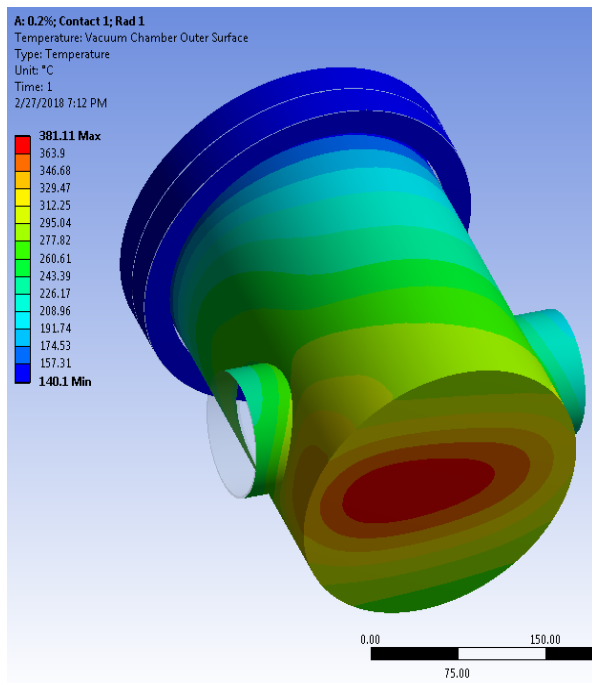


Figure 5: Thermal Analysis results of XPD BRC2 (AZM0008 Rev2) vacuum vessel outer surface

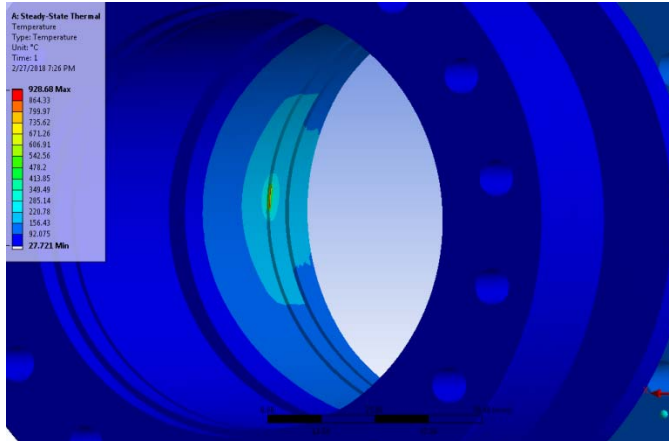


Figure 6: Thermal Analysis of STW vacuum vessel

MCO090



Tungsten Alloys

FMB Oxford
Unit 1 Ferry Mills
Osney Mead
Oxford
OX2 0ES

Unit 10-12 Beacon Court
Pitstone Green Business Park
Quarry Road, Pitstone
Leighton Buzzard
LU7 9GY

Tel: +44 (0) 1296 664245
Fax: +44 (0) 1296 664201
E-mail: sales@tungsten-alloys.co.uk
Web: www.tungsten-alloys.co.uk

CERTIFICATE OF CONFORMITY

Certificate No: TACOC 05166 Despatch No: TAD 05166
Your O/No: 5084 Despatch Date: 14 August 2013
Our O/No: 8175 *W001265*

ITEM	DESCRIPTION	QTY ORDERED	UNIT	QTY DESPATCHED	BATCH NO
	TAM 2000 - 95% W - 4% NI - 1% Cu 18g/cm³				
1	TAM 2000 - XPD BRC2 Tungsten Block ACC0031 Rev02	1	ea	1	8175/072270
2	TAM 2000 - XPD BRC Tungsten Shield ACC0077 Rev02	1	ea	1	8175/072270

REMARKS

Certified that the whole of the materials and/or parts detailed hereon furnished against this purchase order, unless otherwise stated above, were manufactured and supplied in conformance with all applicable requirements and/or to your drawing.

Signed:  14 August 2013
For and on behalf of Tungsten Alloys

Figure 7: Certificate of Conformance for Tungsten material

